The Role of Antihydrogen Formation in the Radial Transport of Antiprotons in Positron Plasmas

Svante Jonsell[1], Mike Charlton[2] and Dirk van der Werf [2,3]

[1]*Department of Physics, Stockholm University, SE-10691, Stockholm, Sweden*
[2]*Department of Physics, College of Science, Swansea University, Swansea SA2 8PP, UK*
[3]*IRFU, CEA, Saclay, 91191, Gif-sur-Yvette Cedex, France*

E-mail: jonsell@fysik.su.se

Simulations have been performed of the radial transport of antiprotons in positron plasmas under ambient conditions typical of those used in antihydrogen formation experiments in Penning traps. The simulations were performed using classical trajectories of both antiprotons and surrounding positrons with randomized initial conditions. In addition, friction and fluctuation forces on the antiproton due to interaction with the positron plasma were included. This gives rise to both axial and radial diffusion of the antiprotons at a rate given by the magnetic field, the positron temperature and the plasma density, and the parameter range explored includes at least two values of each. As the antiprotons travel through the positron plasma they undergo repeated cycles of antihydrogen formation and re-ionization. We find that when these effects are added to the simulations the properties of the radial diffusion alter dramatically, even changing from normal to anomalous diffusion. We attribute this to the azimuthal drift of the antiprotons in the crossed magnetic (from the trap) and electric fields (from the space charge of the plasma). When the antiprotons are neutralised through antihydrogen formation this drift is temporarily interrupted, and the antiproton (carrying a positron) continues in the tangential direction. On average this motion will give an increase of the radial position of the antiproton, relative the trap axis. At low positron plasma temperatures, repeated cycles of antihydrogen formation and destruction are the dominant source of radial (cross magnetic field) transport. On time scales of a few milliseconds (depending on plasma parameters) the antiprotons will reach the edge of the cylindrical plasma, where the radial transport will cease, and thus the antiprotons will accumulate there.

KEYWORDS: antihydrogen, antiprotons, transport, positron, plasma

1.   Introduction

Antihydrogen ($\bar{\text{H}}$) is nowadays routinely produced in copious quantities by several experiments located at the Antiproton Decelarator at CERN [1]. Recent advances include trapping of antihydrogen atoms in magnetic traps [2–5], the creation of an antihydrogen beam [6,7], a first investigation of its internal structure [8], a rudimentary investigation of its gravitational mass [9], and high-precision measurements of its charge [10,11].

Still, there is a strong desire to be able to produce antihydrogen at lower kinetic energies, which would help to increase the trapping rate, which in turn would make high-precision studies of its properties easier. Typically, out of 10,000:s antihydrogen produced in an experimental cycle, less than a handful get trapped. This is due to the difference in energy scale between the charges particles (eV) and the depth of the magnetic trap (~ 0.5 K for ground-state antihydrogen).

In almost all antihydrogen experiments to date, the charged particles are held in a Penning, or Penning-Malmberg, trap [12–14]. In these the charged particles are collected, manipulated, and mixed to form the anti-atoms. Such traps have a cylindrical geometry, and employ strong magnetic fields

(typically of tesla strength) for radial confinement of the charged species, as the field is directed along the axis of a series of electrodes, with the latter suitably electrically biassed to provide the axial confinement. In this work we shall employ coordinates such that $\hat{\mathbf{z}}$ corresponds to the direction along the axis of the trap, and $\hat{\mathbf{x}}$, $\hat{\mathbf{y}}$ span the plane perpendicular to the axis. Hence, including only the magnetic field from the Penning trap (i.e., omitting the fields from any magnetic trap present) it has the form $\mathbf{B} = B\hat{\mathbf{z}}$. To date, almost all antihydrogen experiments have involved mixing antiprotons ($\bar{p}$) and positrons (e^+) in a so-called nested Penning trap environment [15] in which typical e^+ cloud/plasma temperatures, T_e, have been below 100 K (though this parameter was not always directly measured) and with densities in the range from $n_e = 10^{13}$ to 10^{15} m^{-3}. The electric field along the trap axis vanishes, but because of the self-charge of the plasma there is an electric field of the form

$$\mathbf{E} = \frac{n_e e \mathbf{r}}{2\epsilon_0} = E\hat{\mathbf{r}}, \tag{1}$$

which is radial, $\mathbf{r} = r\hat{\mathbf{r}}$, in nature with e the elementary charge and ϵ_0 the permittivity of free space.

The antihydrogen atoms are formed by letting the $\bar{p}$:s pass through a trapped plasma of positrons. The dominant formation mechanism is believed to be three-body recombination, as

$$\overline{p} + e^+ + e^+ \rightarrow \overline{\mathrm{H}}^{**} + e^+. \tag{2}$$

The anti-atoms formed through reaction 2 are very weakly bound (by of the order of $k_B T_e$ where their excited nature is denoted by the double-star superscript) [16–18], and are thus strongly influenced by the electric and magnetic fields in the trap. These weakly bound antihydrogen then undergo further collisions with positrons, which may either re-ionize them,

$$e^+ + \overline{\mathrm{H}}^{**} \rightarrow \overline{p} + e^+ + e^+, \tag{3}$$

or alternatively increase their binding energy, which eventually leads to an anti-atom which is stable against re-ionization by further collisions

$$e^+ + \overline{\mathrm{H}}^{**} \rightarrow \overline{\mathrm{H}}^* + e^+. \tag{4}$$

2. Simulations

A number of authors have performed simulations and theoretical analyses of various aspects of antihydrogen formation, as applied to the experimental situations [19–30], and as summarised by Robicheaux [17]. The methodology used here has previously been described in [18, 30], so we give only a very brief outline.

The trajectories of all particles are calculated classically using the full equations of motion, including the interaction with magnetic and electric fields, as well as with other particles present in the simulation. Only a single antiproton is simulated at a time, and the number of positrons present is determined by defining a box which moves with the antiproton, letting positrons enter through the sides of the box at a rate determined by the positron density n_e, the positron temperature T_e, and the velocity of the antiproton. When a positron trajectory leaves the box the particle is removed from the simulation. In all simulations reported here, the antiprotons were initiated on the axis of the trap, with a velocity taken randomly from the kinetic distribution characteristic of the temperature of the plasma (i.e. it is assumed that the antiprotons have already thermalised with the positron plasma). Typically 20,000 antiproton trajectories were calculated for each set of parameters, in order to obtain sufficient statistics.

We also include a friction force due to the antiproton interaction with the positron plasma. The same interaction also gives rise to random recoils, which is expressed through a diffusive force with

zero time-average $\langle F(t) \rangle = 0$, but non-zero higher-order moments, e.g. $\langle F(t)^2 \rangle \neq 0$. The balance between these two forces keeps the antiprotons at the same temperature as the positrons. We use a form for this force taken from [31]. Throughout the simulation we keep track of the radial position $r(t)$ of the antiprotons, where $r = 0$ corresponds to the axis of the trap.

3. Particle motion in Penning traps

3.1 Free particles

The force on a particle with charge q ($q = +e$ for e^+:s, and $q = -e$ for $\bar{p}$:s) and mass M within the trap is

$$\mathbf{F} = q(\mathbf{v} \times \mathbf{B} + \mathbf{E}) = M\omega_c(v_x\hat{\mathbf{y}} - v_y\hat{\mathbf{x}}) + M\frac{q}{e}\frac{\omega_{\text{pl}}^2}{2}(x\hat{\mathbf{x}} + y\hat{\mathbf{y}}), \tag{5}$$

where $\mathbf{v}$ is the velocity of the particle, and with

$$\omega_c = -\frac{qB}{M}, \tag{6}$$

its cyclotron frequency, and

$$\omega_{\text{pl}} = \sqrt{\frac{e^2 n_e}{M\epsilon_0}} \tag{7}$$

the plasma frequency. The equations of motion have two solutions,

$$\Omega_\pm = \frac{\omega_c}{2}\left[1 \pm \sqrt{1 + 2\frac{q}{e}\frac{\omega_{\text{pl}}^2}{\omega_c^2}}\right]. \tag{8}$$

That is, in the plane perpendicular to the magnetic field, the motion of the particle will be the superposition of two circular motions with the frequencies above. For typical experimental parameters $\omega_c \gg \omega_{\text{pl}}$, and the radius of the Ω_+ motion is much smaller than that of the Ω_- motion. That means that the trajectory of the particle is to the leading order approximation a rapid circular motion with frequency $\Omega_+ \simeq \omega_c$, i.e. the cyclotron motion, superposed on a much slower orbit with frequency

$$\Omega_- \simeq \frac{q}{e}\frac{\omega_{\text{pl}}^2}{2\omega_c} = -\frac{en_e}{2\epsilon_0 B} = -\frac{E}{B}\frac{1}{r}, \tag{9}$$

around the axis of the trap. Note that to leading order Ω_- is independent of q and M. Hence, when the condition $\omega_c \gg \omega_{\text{pl}}$ is satisfied, positrons and antiprotons will slowly co-rotate with the same velocity. The temperature of the particles is then defined by the energy stored in the respective cyclotron motions relative this rotating frame of reference. This rotation will, however, add to the kinetic energy of the antiprotons in the laboratory frame. Antihydrogen formed by the reaction 2 will to a very good approximation inherit its kinetic energy from the antiproton. Thus, in order to form trappable antihydrogen, this motion should be minimised. One way to do this is to reduce Ω_- through the plasma density n_e, or by increasing B. However, both quantities have practical limitations. (In the case of n_e due to the three-body formation rate, which is proportional to n_e^2.) Another way to reduce the speed $v_T = \Omega_- r$ of this motion is to keep the antiprotons close to the trap axis. Therefore, effects leading to radial drift of antiprotons, such as the mechanisms investigated in this article, are undesirable.

Examining the condition of validity for this approximation we find that $\omega_c \gg \omega_{\text{pl}}$ entails that (for the antiproton mass)

$$\frac{B}{1\text{T}} \gg 0.04\sqrt{\frac{n_e}{10^{13}\text{m}^{-3}}}, \tag{10}$$

3

meaning that for very high densities and ∼ Tesla magnetic fields this approximation will not hold. As an example, $n_e = 10^{15}$ m^{-3}, and $B = 1$ T gives $\omega_{\mathrm{pl}}/\omega_c \simeq 0.4$. Expanding equation (8) to next order we find that the relative leading correction is $-\omega_{\mathrm{pl}}^2/(2\omega_c^2)$, i.e. for the numbers above ∼ -8%. In contrast, for the positrons, owing to their lighter mass, the corresponding correction is negligible. Thus, in the frame of the positrons the antiprotons will be rotating with a speed $-\omega_{\mathrm{pl}}^4 r/(4\omega_c^3)$, where r is the radial position in the trap. If this mismatch between the speeds is small enough the positrons are likely to drag the antiprotons with them, because of the interaction between the particles. However, if the mismatch is too large it is likely that the rate of antihydrogen formation is reduced. In order to avoid these rather complicated effects, we have limited our simulations to positron densities $n_e \leq 10^{15}$ m^{-3}. However, at the largest densities investigated we find some small anomalies, which we tentatively attribute to this effect. This will be the subject of further investigation.
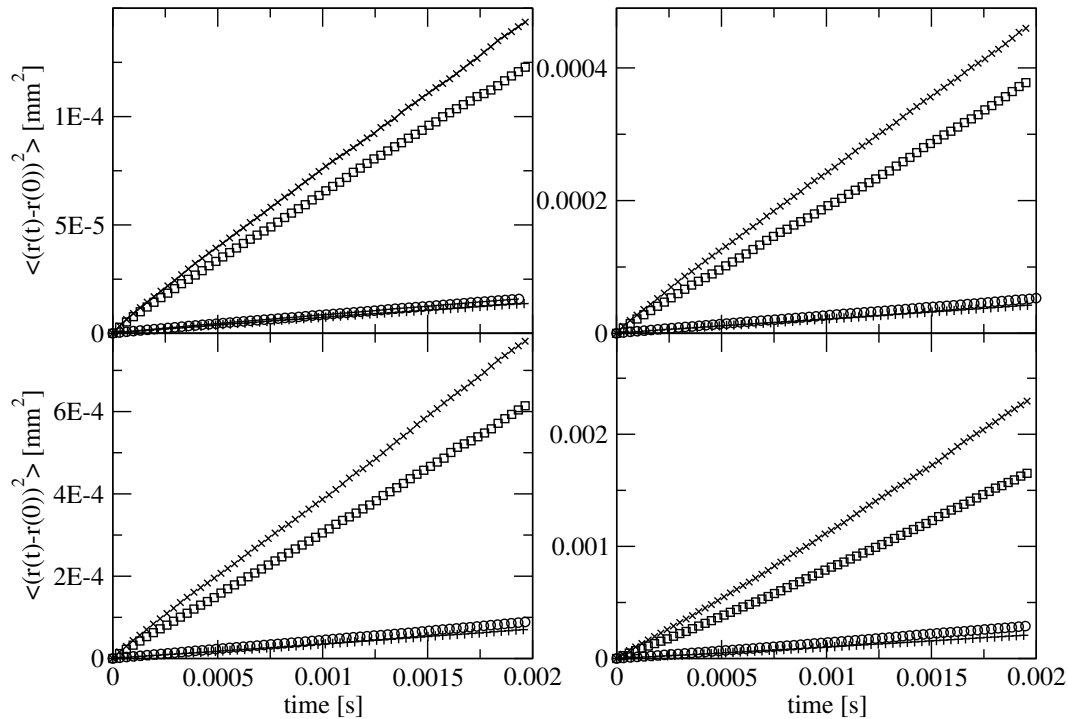

Fig. 1. Time evolution of the average radial position of the antiproton, including the thermal diffusion. The positron densities are $n_e = 10^{13}$ m^{-3} (top left), $n_e = 5 \times 10^{13}$ m^{-3} (top right), $n_e = 10^{14}$ m^{-3} (bottom left), and $n_e = 5 \times 10^{14}$ m^{-3} (bottom right). Symbols: $T_e = 30$ K, $B = 1$ T (crosses), $T_e = 15$ K, $B = 1$ T (squares), $T_e = 30$ K, $B = 3$ T (circles), and $T_e = 15$ K, $B = 3$ T (plusses).

In the co-rotating frame the antiprotons will collide with positrons. From each collision the trajectory of the antiproton will be randomly perturbed, leading to a radial diffusion dependent on temperature. This diffusion is strongly counteracted by the pinning of the charged particles to the magnetic field lines. We have performed a number of simulations of this "thermal diffusion", some of the results can be found in figure 1. We find that the time evolution can be very well fitted to the form $\langle (r(t) - r(0)^2 \rangle = 2Dt$, where D is a diffusion coefficient, as is characteristic of Brownian motion. We find that the rate of diffusion grows with density, and slightly with temperature, as would be expected. The main effect, though, is that radial thermal diffusion is much less significant for larger magnetic fields. This is clearly an effect of a harder pinning of the charged particles to the magnetic field lines.

The corresponding diffusion coefficients as a function of positron density n_e are displayed in
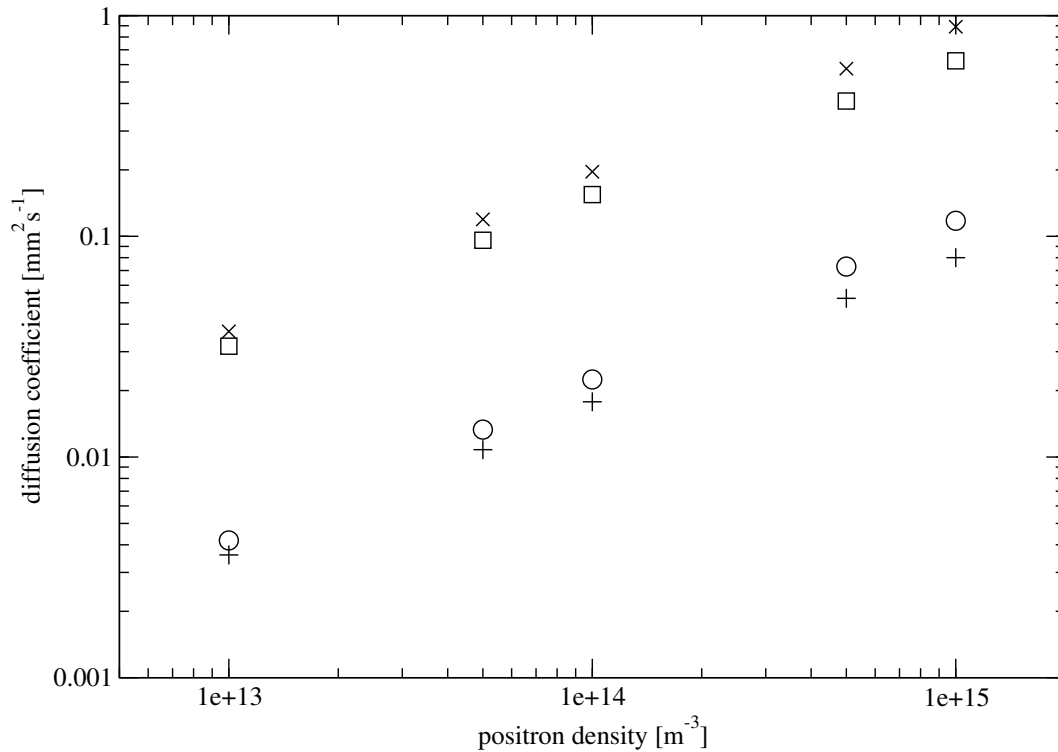
Fig. 2.   Diffusion coefficients as a function of positron density for different positron temperatures and magnetic fields: T_e = 30 K, B = 1 T (crosses), T_e = 15 K, B = 1 T (squares), T_e = 30 K, B = 3 T (circles), and T_e = 15 K, B = 3 T (plusses).

figure 2. We find that for all sets of parameters the density dependence is well fitted by $D \propto n_e^a$, with a taking values between 0.64 and 0.69. Finally, the diffusion coefficient over a more extended range of temperatures is plotted in figure 3, for the parameters $n_e = 10^{15}$ m^{-3}, and B = 3 T. We find that the data points up to 30 K are well fitted by the expression $D = 0.0125T^{0.66}$.

3.2   Effects from antihydrogen formation

We now add the possibility of antihydrogen formation through the reaction 2. This means that the antiprotons will cycle between their bare charged state, and a neutral state inside an antihydrogen atom. On rare occasions the antihydrogen will become deeply bound, and hence drift more or less unperturbed out from the positron plasma, where it may either be detected as it hits the surrounding electrodes, or trapped, if a magnetic trap is present and its kinetic energy small enough. While charged the antiprotons will follow the circular motions described above. However, when neutralised the antiproton will not feel the magnetic or electric forces, but will continue in a straight trajectory, with a velocity close to the antiproton velocity before formation. As described above this velocity is the combination of a thermal cyclotron motion and a rotation around the trap axis. While the former is random in direction, the latter will for a given radius r in the trap, always give an added tangential component to the velocity with speed v_T.

While the antiproton is bound inside an antihydrogen it may therefore "jump" to a different trap radius. We define the jump length Δr as the difference between the radial position when the antihydrogen is ionised and that at which it was formed. If there is only the thermal motion the distribution of such jumps will be symmetric around $\Delta r = 0$, but the addition of v_T in the tangential direction produces a bias towards $\Delta r > 0$. Simulated distributions of such jumps are shown in figure
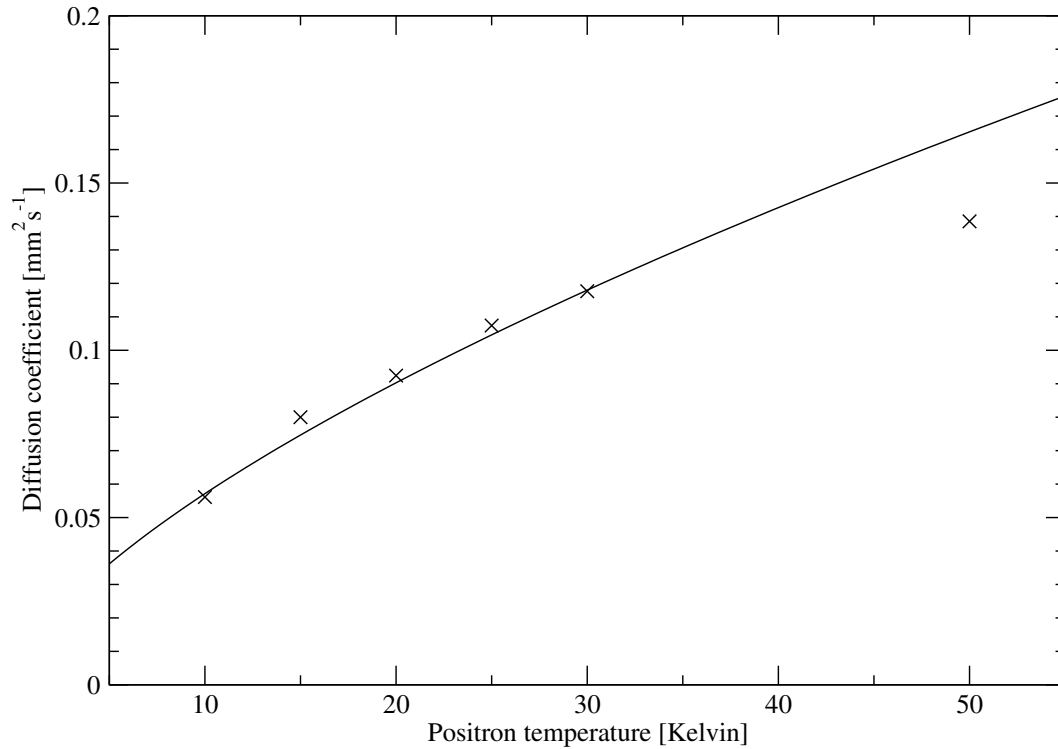
5

Fig. 3. Diffusion coefficients as a function of positron temperature, the density is $n_e = 10^{15}$ m^{-3}, and the magnetic field $B = 3$ T. The line is a fit (see text).

4, for two different densities. It is clear that there is a bias towards $\Delta r > 0$. For the lower density there is a clearly visible tail extending to large jumps in the positive direction.

It turns out that this long-range tail makes the distribution of jumps non-normalisable. In terms of the simulations that means that we cannot form an ensemble average of $r(t)$, because a few very long jumps will distort the average. We therefore introduce a cut-off radius $r_c = 1$ mm. Any antiproton, bare or bound in antihydrogen, which passes this radius is removed from the simulation, and $\langle r(t) \rangle$ is formed only from antiprotons with $r(t) < r_c$. This means that $\langle r(t) \rangle$ may approach, but never pass r_c. It also means that as t increases the average will be formed by fewer antiprotons, leading to increasing statistical uncertainty. Physically, r_c can be thought of as the radius of the positron plasma.

Our final results, including both the thermal diffusion and antihydrogen formation, are summarised in figure 5. We see that while the thermal diffusion depends strongly on the magnetic field, the antihydrogen formation mechanism is much less field-dependent and more temperature dependent (since the antihydrogen formation rate is strongly temperature dependent). At $T_e = 15$ K and $n_e = 10^{15}$ m^{-3} the average radial position grows to close to r_c for both fields, while at $T_e = 30$ K the average never gets close to this radius within the 2 ms duration of the simulation. For $T_e = 30$ K, $B = 3$ T and $n_e = 10^{13}$ m^{-3} we also see that the distribution from the full simulation follows the thermal-only distribution until it suddenly makes a jump around $t \simeq 1.8$ ms. This demonstrates how a jump from a single antiproton can strongly affect the average, when the average is small. The discontinuity in the distribution is of course not statistically significant. For all other parameters the radial drift including antihydrogen formation greatly exceeds the thermal-only drift. Another striking difference is that the drift due to antihydrogen formation is ballistic i.e. $\langle r(t) - r(0) \rangle \propto t$, whereas, as pointed out above, for thermal drift $\langle r(t) - r(0) \rangle = 0$, while $\sqrt{\langle (r(t) - r(0))^2 \rangle} \propto \sqrt{t}$.
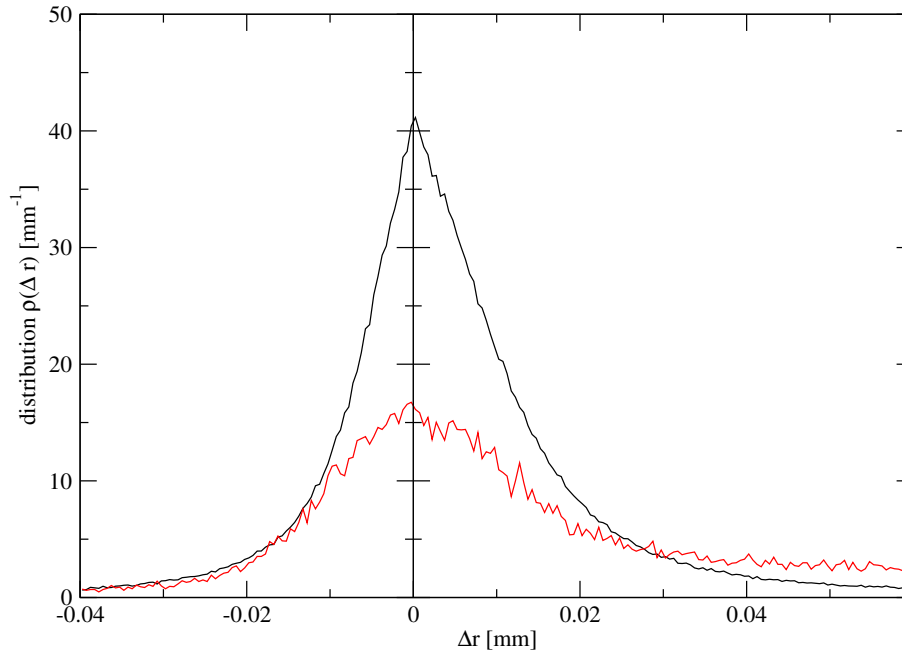
Fig. 4.   Distribution of jumps in radial position Δr of an antiproton, when antihydrogen is formed. Temperature $T_e = 15$ K, magnetic field $B = 1$ T and two different densities $n_e = 10^{15}$ m^{-3} (black), and $n_e = 10^{14}$ m^{-3} (red). The central part of the distribution is mainly due to the thermal motion stored in the cyclotron orbits of the antiprotons, which is inherited by the antihydrogen upon formation. It is thus symmetric around zero. The long tail in the positive direction is due to the extra tangential velocity arising from the $\mathbf{E} \times \mathbf{B}$ drift.

4.   Conclusions

We have found that when antiprotons move through a positron plasma trapped in a Penning trap, they drift towards larger radii. We investigate two mechanisms for this drift, thermal diffusion, and neutralisation. Since the latter has its origin in the process of antihydrogen formation itself, it is unavoidable that it arises in any antihydrogen experiment using this kind of trap. We investigate time scales for these processes, and find that which of the two mechanisms that dominates is strongly parameter dependent. However, as the positron temperature is lowered and density is increased the antihydrogen formation mechanism rapidly grows in importance. In reference [30] we have outlined a simple analytical model to explain this dependence.

We note that experimental observations from the ATHENA experiment have been interpreted as indication of a similar antiproton drift, though arising from a somewhat different mechanism [32].

5.   Acknowledgements

References

[1] T. Eriksson: Hyperfine Interact. **194** (2009) 123.
[2] G. B. Andresen et al.: Nature **468** (2010) 673.
[3] G. B. Andresen et al.: Nature Phys. **7** (2011) 558.
[4] G. B. Andresen et al.: Phys. Lett. B **695** (2011) 95.
[5] G. Gabrielse et al.: Phys. Rev. Lett. **108** (2012) 113002.
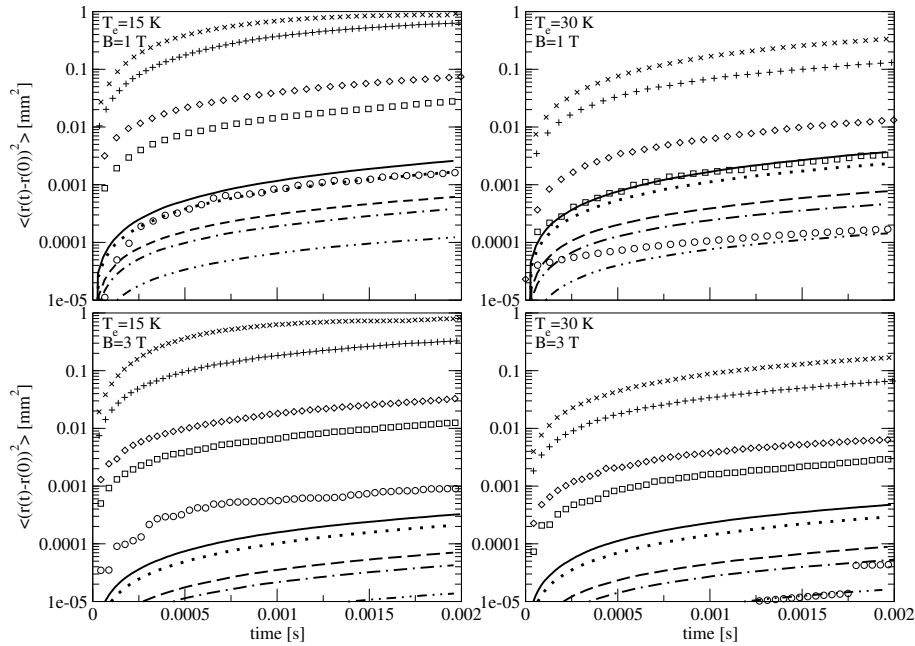[6] Y. Enomoto et al.: Phys. Rev. Lett. **105** (2010) 243401.

Fig. 5. Time evolution of the average radial position of the antiproton (including $\bar{\mathrm{H}}$ formation), assuming a plasma radius of $r_c = 1$ mm. The values for the plasma temperature T_e and the magnetic field B are indicated in each panel. The symbols represent different plasma densities, from above $n_e = 10^{15}$ m^{-3} ($\times$), $n_e = 5 \times 10^{14}$ m^{-3} (+), $n_e = 10^{14}$ m^{-3} (open diamond), $n_e = 5 \times 10^{13}$ m^{-3} (open square), and $n_e = 10^{13}$ m^{-3} (open circle). For comparison we also include the results including only thermal diffusion on the same scale. These are $n_e = 10^{15}$ m^{-3} (solid line), $n_e = 5 \times 10^{14}$ m^{-3} (dotted line), $n_e = 10^{14}$ m^{-3} (dashed line), $n_e = 5 \times 10^{13}$ m^{-3} (dash-dot line), and $n_e = 10^{13}$ m^{-3} (dash-dot-dot line).

[7] N. Kuroda et al.: Nature Commun. **5** (2014) 3089.

[8] C. Amole et al.: Nature **483** (2012) 439.

[9] C. Amole et al.: Nature Commun. **4** (2013) 1875.

[10] C. Amole et al.: Nature Commun. **5** (2014) 3955.

[11] M. Ahmadi et al.: Nature **529** (2016) 373.

[12] F. H. Major, V. N. Gheorge, and G. Werth: *Charged Particle Traps: Physics and Techniques of Charged Particle Field Confinement* (Springer, Berlin, 2005).

[13] P. K. Ghosh: *Ion Traps* (Clarendon Press Oxford, 1995).

[14] L. S. Brown and G. Gabrielse: Rev. Mod. Phys. **58** (1988) 233.

[15] G. Gabrielse, S. L. Rolston, L. Haarsma, and W. Kells: Phys. Lett. A **129** (1988) 38.

[16] M. H. Holzscheiter, M. Charlton, and M. M. Nieto: Phys. Rep. **402** (2004) 1.

[17] F. Robicheaux: J. Phys. B: At. Mol. Opt. Phys. **41** (2008) 192001.

[18] S. Jonsell, D. P. van der Werf, M. Charlton, and F. Robicheaux: J. Phys. B: At. Mol. Opt. Phys. **42** (2009) 215002.

[19] F. Robicheaux and J. D. Hanson: Phys. Rev. A **69** (2004) 010701.

[20] F. Robicheaux: Phys. Rev. A **70** (2004) 022510.

[21] T. Pohl, H. R. Sadeghpour, and G. Gabrielse: Phys. Rev. Lett. **97** (2006) 143401.

[22] C. E. Correa, J. R. Correa, and C. A. Ordonez: Phys. Rev. E **72** (2005) 046046.

[23] S. X. Hu, D. Vrinceanu, S. Mazevet, and L. A. Collins: Phys. Rev. Lett. **95** (2005) 163402.

[24] S. G. Kuzmin and T. M. O'Neil: Phys. Rev. Lett. **92** (2004) 23401.

[25] S. G. Kuzmin and T. M. O'Neil: Phys. Plasmas **12** (2005) 012101.

[26] D. Vrinceanu, S. X. Hu, S. Mazevet, and L. A. Collins: Phys. Rev. A **72** (2005) 042503.

[27] F. Robicheaux: Phys. Rev. A **73** (2006) 033401.

[28] T. Topçu and F. Robicheaux: Phys. Rev. A **73** (2006) 043405.

[29] D. Vrinceanu, B. E. Granger, R. Parrott, H. R. Sadeghpour, L. Cederbaum, A. Mody, J. Tan, and G. Gabrielse: Phys. Rev. Lett. **92** (2004) 133402.
[30] S. Jonsell, M. Charlton, and D. P. van der Werf: J. Phys. B: At. Mol. Opt. Phys. **49** (2016) 134004.
[31] H. B. Nersisyan, M. Walter, and G. Zwicknagel: Phys. Rev. E **61** (2000) 7022.
[32] E. Lodi Rizzini, L. Venturelli, and N. Zurlo: Hyperfine Interact. **193** (2009) 313.